Investigating the Behaviours of Quantum States and Spectra for Gases and Dyes

October 7, 2025

Aarya Shah 1010871157, Sara Parvaresh Rizi 1010913451

Abstract

This experiment used emission spectroscopy to investigate the quantum energy levels of gases and solutions. A PASCO spectrometer was calibrated using Hg lines and then used to record the spectra of hydrogen, helium, and an unknown gas. Bohr's model accurately predicted hydrogen's Balmer series wavelengths, with all measured values within 1% of theoretical predictions and within experimental uncertainty [1]. The model failed for helium due to its multi-electron structure. The unknown gas was identified as likely Krypton based on spectral line matching, with a peak at around 774 nm, and differences in peak wavelengths of under 5%. Analysis of dyes confirmed the complementary relationship between absorption and transmission, and a yellow dye was deemed unsuitable for photovoltaics due to its high band gap (~3 eV).

1. Introduction

Atoms emit light at specific, discrete wavelengths when their electrons transition between quantized energy levels. This phenomenon is described by the Rydberg formula and, for hydrogen, accurately modelled by the Bohr model of the atom. The energy of an emitted photon is given by:

$$E = \frac{hc}{\lambda} = R_H\left(\frac{1}{m^2} - \frac{1}{n^2}\right) \quad (1)$$

Where h is Planck's constant, c is the speed of light, λ, R_H is the Rydberg constant, and m and n are the principal quantum numbers of the energy levels involved [2]. The purpose of this experiment was to verify the quantized energy level model by measuring the emission spectrum of hydrogen and comparing it to the theoretical Balmer series; second, to test the limits of this model by analyzing the spectrum of helium, a multi-electron atom; third, to apply these principles to identify an unknown gas based on its emission signature; and fourth, to investigate the absorption, transmittance, and fluorescence of dye solutions, determining their colour properties and assessing the photovoltaic potential of a yellow dye based on its band gap.

2. Materials and Methods

The lab was conducted by adhering to the outlines in the 'Quantum States and Spectra' manual [2]. The lab is split into 3 parts: calibration, investigating properties of the gases, and assessing the absorbance of solutions.

2.1. Materials

- PASCO Wireless Spectrometer PS-2600 connected to the PASCO software
- Fibre optic cables and probes
- Gas discharge tubes (Hg, H, He)
- Cuvettes with different solutions
- High-voltage power source

2.2. Methods

The spectrometer was first calibrated using a mercury (Hg) discharge tube. The known wavelengths of Hg's spectral lines [2] (row 2 Table 1), were compared to measured values, and a linear correction was applied to all subsequent data. The specifications for using PASCO are taken from [2], found in Appendix 1. The probe distance and software smoothing settings were optimized for each measurement to maximize signal intensity and clarity while minimizing noise.

The emission spectra of Hydrogen (Figure 3), Helium (Appendix 5), and the unknown gas (Figure 4) were then recorded. For the dye analysis, the spectrometer was calibrated to distilled water. The absorption and transmission spectra of the blue, green, and red dyes were measured under white light. The fluorescence of the yellow dye was then examined under 405 nm and 500 nm excitation to determine its absorption edge and calculate its band gap energy.

3. Data and Analysis

3.1. Calibration of the device

All error readings of the spectrometer were 3nm [2]. Using the linear fit in Figure 1 from the values input into Table 1, the spectrometer wavelengths were calibrated to $\lambda_{true} = (1. \pm 0.) * \lambda_{measured} (-10. \pm 13)$, where the slope uncertainty rounds to 0. A reduced chi-squared analysis [3][4] was conducted for goodness of fit, yielding a value of 4.. From error propagation for our energies, the energy errors were in the order of 10^{-2}, rounding to ± 0. This is statistically insignificant and is discarded from our table. All error values and plots in the report are from the code in Appendix 6.

Color	Violet	Violet	Blue	Green	Yellow	Yellow
Expected λ (nm)	404.6565	407.7837	435.8328	546.0735	576.9598	579.0663
Expected energy (eV)	3.0305	3.0848	2.8243	2.2916	2.1713	2.1439
Experimental λ (nm)	409. ± 3	402. ± 3	439. ± 3	541. ± 3	571. ± 3	579. ± 3
Experiment energy (eV)	3.	3.	3.	2.	2.	2.

Table 1: Expected wavelengths (nm) and energies (eV) compared to experimental wavelengths (nm) and energies (eV). The Experimental λ row holds the same error of ±3.nm from the resolution of the PASCO device.

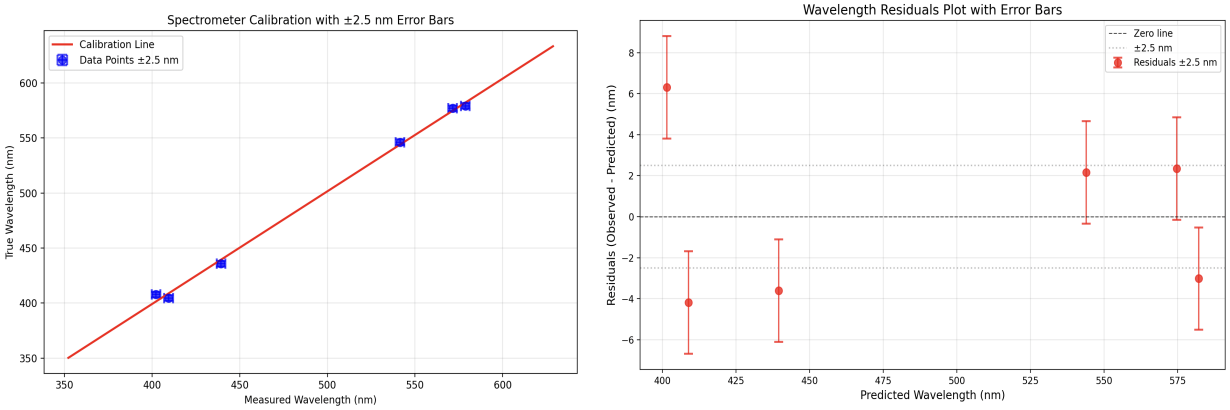

Figure 1: A linear fit $\lambda_{true} = (1.) * \lambda_{measured} + (-10. \pm 13)$ nm on the measured and experimental wavelengths (left) and a resulting residual plot (right). The mean residual is 2. nm, with standard deviation 4.

Similarly, energy calibration $E_{true} = (1.) * E_{measured}\ eV$ also yielded poor fit statistics. The reduced chi-squared for this measurement was also 4. The plots for the linear fit and residual plot are in Figure 2.

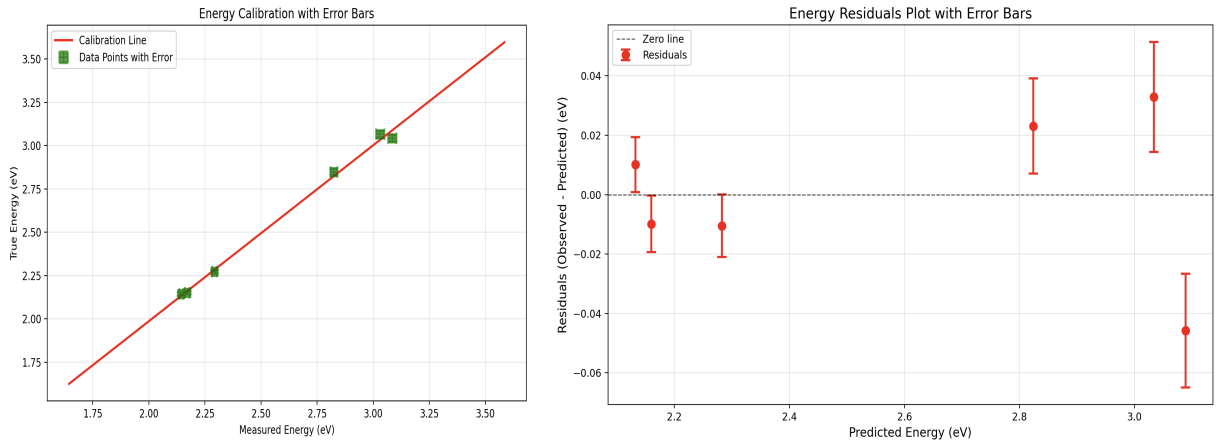

Figure 2: A linear fit $E_{true} = (1.) * E_{measured}$ eV applied to the calculated energies(left) and a residual plot of the results (right). The mean residual is 0. eV, and the standard deviation rounds to 0. as well.

3.2. Quantum States of Hydrogen

The wavelengths of Hydrogen were measured at its strongest emission lines to determine its quantized energy levels, and recorded in Table 2. The energies were calculated using Equation (2), where n=3,4,5, and Z=1 for the Hydrogen atom's proton [2].

$$E_n = -\left(\frac{Z^2 k_e e^2}{2n^2 a_0}\right) \sim \left(\frac{-13.6Z^2}{n^2}\right) eV \qquad (2)$$

This experimental data was compared to the expected energies of the spectral lines of the Balmer series (Hydrogen's characteristic spectrum) with different n (see Equation (3)) [2].

$$hf = \frac{hc}{\lambda} = E = R_{EH}\left(\frac{1}{2^2} - \frac{1}{n^2}\right) \qquad (3)$$

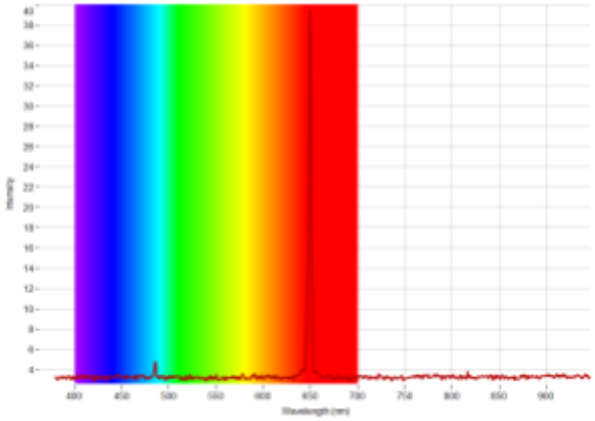

Figure 3: Graph of the Hydrogen Tube Spectra

The measured wavelengths for hydrogen's Balmer series (n=3,4,5,6 → 2) are shown in Table 2. The calculation of error for the experimental wavelengths is outlined in Appendix 4, taking into account the slope error, intercept error, and spectrometer resolution. The percent error is shown for experimental and expected wavelengths. We incorporated up to n=6 energy levels because hydrogen has four characteristic lines [6].

Energy Levels (n)	Energy (E_n) of n from Equation (2)	Expected Spectral Line Energy (eV) from Equation (1)	Expected Spectral Line λ in nm from Equation (3)	Experimental λ (after calibration) in nm	Percent Difference (%) of Experimental λ and Expected λ to 2 Decimals
3	-1.51	1.89	656.45	652. ± 24.	0.68
4	-0.85	2.55	486.55	486. ± 20.	0.11
5	-0.54	2.86	433.81	430. ± 19.	0.88
6		3.02	410.83	410. ± 18.	0.20

Table 2: Quantum State Energies (E_n [eV]) of energy levels n=3, 4, 5, and Theoretical and Calibrated Energies (E [eV]) and Wavelengths (λ [nm]) corresponding to energy levels n=3, 4, 5, 6. The percent difference between the expected and experimental wavelengths is shown.

3.2. Transitions of Helium

To examine if Helium was Hydrogen-like or not, we compared its peak wavelength reported at around 588nm [2], and used the Balmer series equation (Equation (3)) to compare theoretical to actual values. The theoretical value was calculated to be around 163 nm, not at all close to 588nm.

On the PASCO spectrometer, we placed our data on a reference of the He spectrum, which gave us data points to compare our wavelengths. The spectroscopy of Helium is shown in Appendix 5. This data is conveyed in Table 3, where energies E_n were calculated with Equation (1).

Electron configuration of the initial state (upper level)	Electron configuration of final state (lower level)	Reference intensity in arbitrary units	Reference wavelength of the emission line, λ_r, nm	Measured wavelength of the emission line λ_{exp} +/- uncertainty, nm	Percent difference between λ_{exp} and λ_r (%). To 2 Decimals	Energy of the quantum state E_n [eV] for energy level n.	Energy of the quantum state E_m [eV] for energy level m.	Selection rules		
								Δn	Δl	ΔJ
1s2p (1)	$1s^2(0)$	1000	58.43339	Not measured	-	21.23268	-24.57	1	1	1
1s3s (1)	1s2p(2)	200	706.5190	703. ± 25.	0.50	1.7561	-3.60	1	-1	-1
1s3p (1)	1s2s(1)	500	388.8648	382. ± 18.	1.77	3.1906	-4.75	1	1	0
1s3d (3)	1s2p (2)	500	587.5621	584. ± 22.	0.61	2.1116	-3.60	1	1	1
1s3d (2)	1s2p (1)	100	667.8151	664. ± 24	0.57	1.8578	-3.35	1	1	1
1s3p (1)	1s2s (0)	100	501.56783	506. ± 20.	0.88	2.4736	-3.95	1	1	1
1s4d (1)	1s2p (2)	200	447.14802	447. ± 19.	0.03	2.7747	-3.60	2	1	-1

Table 3: Electron configuration and permitted transitions in the He atom. The reference wavelengths and intensity are taken from the lab handout, and the only values we input were λ_{exp}, with its error from calibration, and E_n, which was calculated. The errors for λ_{exp} were calculated in the same way as for Table 4.

3.3. Unknown Gas

Figure 4 shows the data with the spectral lines of the unknown gas, with prominent peaks at (764. ± 26.) nm and (815. ± 28.) nm. The results after calibration are in Table 4.

Measured Wavelength $\lambda_{measured}$ (nm)	True Wavelength λ_{true} (nm)	Measured Energy = (1.0)*True Energy E_{true} (eV)
411. ± 3.	409. ± 18.	3.
448. ± 3.	448. ± 19.	3.
550. ± 3.	554. ± 21.	2.
751. ± 3.	764. ± 26.	2.
800. ± 3.	815. ± 28.	2.
817. ± 3.	832. ± 28.	2.

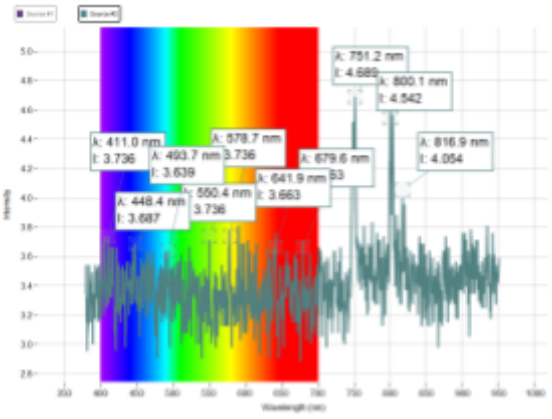

Figure 4: Spectrum of Unknown Gas

Table 4: Calibrated Wavelengths and Energy Values. Errors for the measured wavelengths are all 3nm, from the resolution.

Comparison with reference data (Table 5) showed the strongest correlation with Krypton, which was the only candidate with intense spectral lines beyond 800 nm.

True wavelength λ_{true} of unknown gas (nm) from Table 5	Spectral lines of Krypton from Appendix 2	Percent Difference (%) of Wavelengths between Krypton and Unknown Gas to 2 Decimals	Experimental intensities of spectral lines of unknown gas, in arbitrary units	Relative intensity of experimental wavelengths of the unknown gas
409. ± 18.	427	4.22	3.736	79.676%
448. ± 19.	432	3.70	3.687	78.631%
554. ± 21.	557	0.54	3.736	79.676%
590. ± 22.	587	0.51	3.785	80.720%
645. ± 23.	646	0.15	3.541	75.517%
764. ± 26.	759	0.66	3.614	77.074%
774. ± 27.	769	0.65	4.689	100%
815. ± 28.	810	0.62	4.542	96.9%
832. ± 28.	826	0.73	4.054	86.5%

Table 5: A summary of the Experimental Wavelengths and Intensities of the Unknown gas, compared to the strongest spectral lines of Krypton, the gas believed to be the unknown gas, and the relative intensity of the unknown gas with its highest emission intensity (I=4.689) and wavelength.

From Table 5, the strongest emission line was at 774. ± 27. nm. Compared to the strongest spectrum lines of other gases from the manual appendix, Krypton's lines were the closest. Based on the unique presence of strong lines in the 800 nm range and the overall spectral match, Krypton was identified as the best candidate.

3.4. Transmittance and Absorbance Measurements

Absorbance and transmittance measurements of the blue, (Figure 5), green, and red solutions (Figure 6) are included below, labelled with points of interest like minima, maxima, and points of drastic growth.

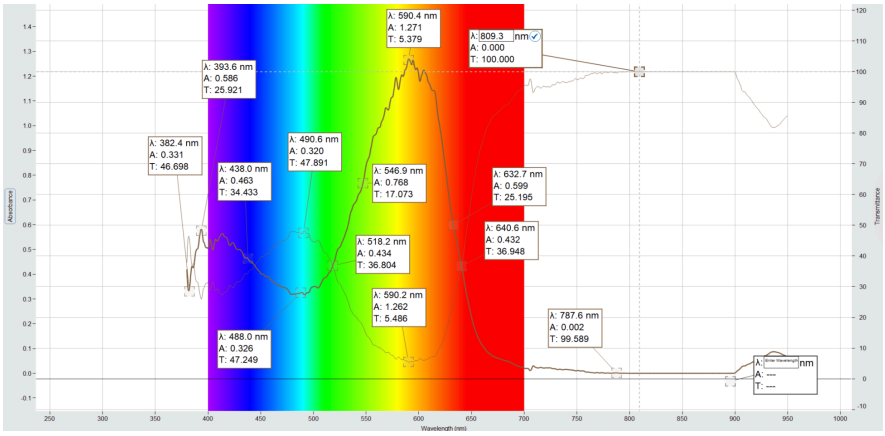

Figure 5: Absorbance and transmittance graph of blue solution, with points of interest labelled.

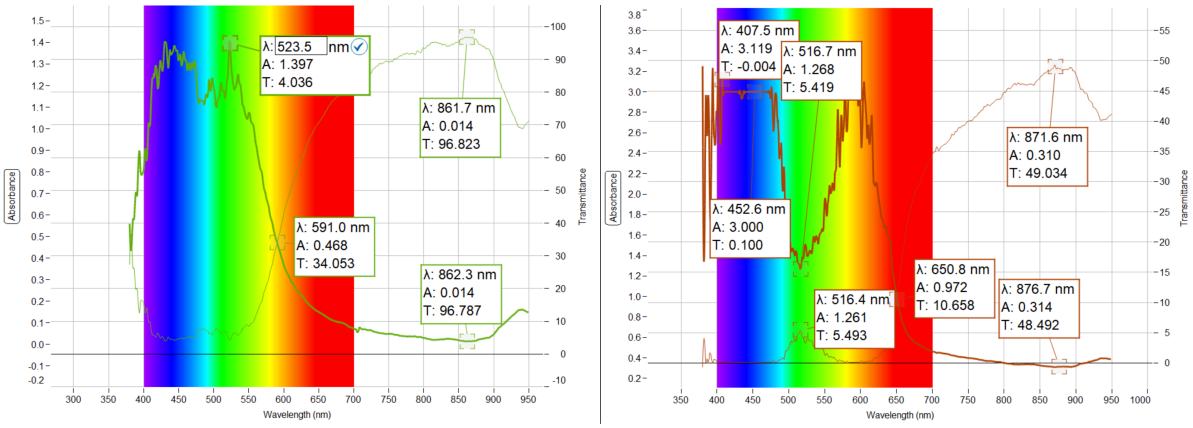

Figure 6: Absorbance and transmittance graph of green (left) and red (right) solutions, with points of interest labelled.

The calculated values of absorbance are summarized in Table 6 for points of interest, using the absorbance equation:

$$A = -\log_{10}(T/100) \quad (4)$$

Color	Special point	Measured Absorbance (A)	Measured Transmittance (T)	Calculated Absorbance (Eq. 6)	Colour most absorbed	Colour most transmitted
Blue	Max T	0.320	47.891	0.320	Red/orange	Blue
	Min T	1.271	5.379	1.269		
	Inflection	0.432	36.948	0.432		
Green	Max T	0.310	49.034	0.310	Blue/red	Green
	Min T	3.119	-0.004	error		
	Inflection	0.972	10.658	0.972		
Red	Max T	0.014	96.823	0.014	Blue/green	Red
	Min T	1.397	4.036	1.394		
	Inflection	0.468	34.053	0.468		

Table 6: Measured and calculated absorbance (A) and Transmittance (T) for some points in blue, green, and red solutions.

The absorption and transmission spectra of the solutions confirmed the principle of complementary colours. Each dye mostly transmitted [12] its own colour and absorbed the complementary colour (e.g., blue dye absorbed orange light). This occurs because photons with energies matching electronic resonances are absorbed.

3.5. Fluorescence

The spectra of the yellow dye with 405nm (purple light) and 500 nm (green light) are in Figures 7 and 8.

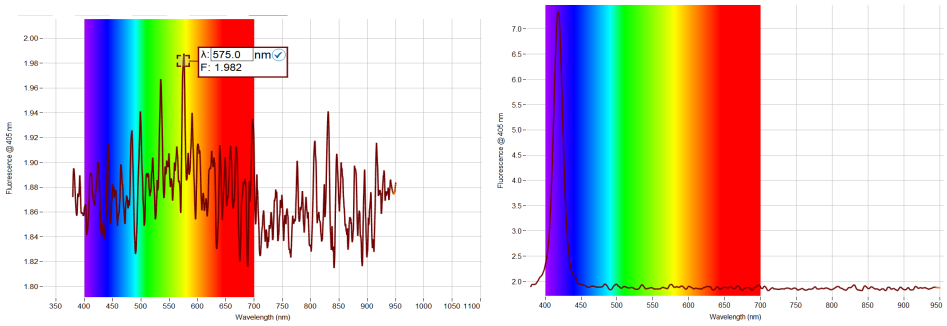

Figure 7. Absorption graph of yellow dye (left) compared to the absorption graph of 405 nm (right).

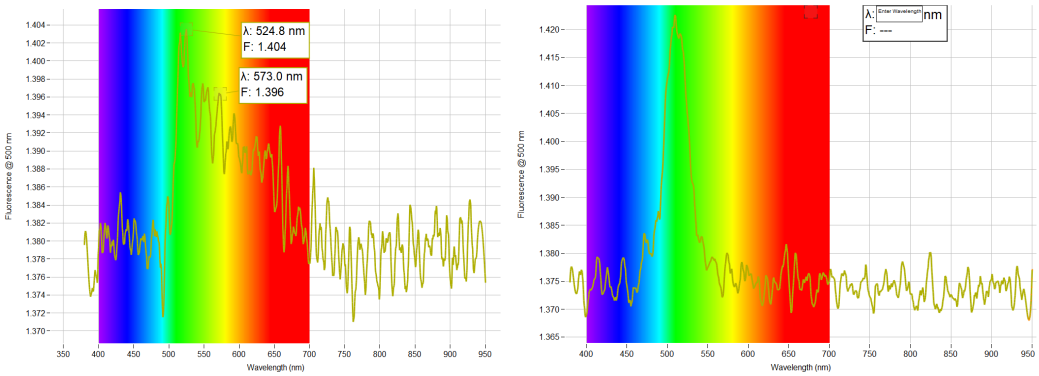

Figure 8. Absorption graph of yellow dye (left) compared to the absorption graph of 500 nm (right).

We noted that although the graph for yellow dye over purple (Figure 7) was very noisy, it makes sense that the peaks would provide a wide range of colours, as purple mixed with yellow gives a brown colour. The fluorescence of yellow dye on green was very noisy too (Figure 8), but yellow and green usually give a lime-green colour, which corresponds to most of the peaks of Figure 8 being closer to green.

Upon testing the yellow dye with fluorescence at 405nm and fluorescence at 500nm, and the absorption edge, Figure 9 shows the absorption graph. The dye's absorption edge was at 387. ± 18. nm, corresponding to an energy band gap of 3. eV using Equation (1).

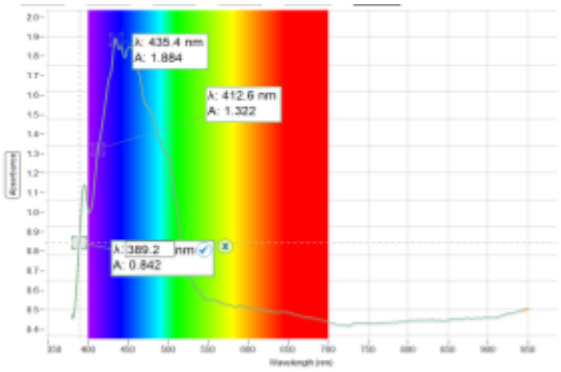

Figure 9: The Absorption Spectrum of a Cuvette with Yellow Dye Inside. This is used to calculate the absorption edge of the dye and determine its photovoltaic properties.

4. Discussion and Conclusion

The experiment successfully demonstrated the principles of atomic emission spectroscopy. The spectrometer was calibrated to $\lambda_{true} = (1. \pm 0.) * \lambda_{measured} (-10. \pm 13)\, nm$ and $E_{true} = (1.) * E_{measured}\, eV$. The large intercept uncertainty and a high reduced chi-squared value of 4. indicate significant systematic error, likely dominant over the stated 3 nm resolution-based statistical uncertainty. This means statistical uncertainties from the resolution inadequately explained the data-model discrepancy and presented dominant systematic errors. The initial setup and optimization were crucial, as we found that signal intensity was maximized when the probe was around 0.5cm away from the discharge tube. Moving it closer lowered the intensity, likely due to reflection and scattering as the probe neared the glass. Furthermore, software smoothing needed adjustment, as oversmoothing artificially flattened spectral peaks, while undersmoothing displayed a lot of high-frequency noise that obscured the spectrometry's features.

The Bohr model proved highly accurate for hydrogen. The measured wavelengths for the Balmer series (n=3,4,5,6 to n=2) all agreed with the theoretical prediction within experimental uncertainty, and percent differences were all under 1%. This strong agreement confirms quantized energy levels in one-electron systems (such as Hydrogen). However, we noticed the relative intensities of the spectral lines varied between the experiments. We hypothesize this is due to several factors: temperature governing excited state populations [7] (Boltzmann distribution), gas density affecting emitter count, transition probabilities (oscillator strength), and detector wavelength sensitivity [5]. We also concluded the characteristic red colour of the hydrogen tube is due to the 656 nm transition (n=3 to n=2) having the highest intensity in the visible spectrum, aligning closely with the tube colour we saw in the lab.

In contrast, the Bohr model failed for Helium. Applying a Hydrogen-like ion equation to an n=3 to n=2 transition gave an expected wavelength of around 163nm, starkly contradicting the highest intensity line being around 588nm. This arises from electron-electron repulsion, spin interactions (Pauli Exclusion), and enhanced nuclear attraction [8], which is not accounted for in the simple Hydrogen-like model, because neutral Helium has two electrons [9]. These factors produce energy level splitting and higher transition energies, explaining helium's complex spectrum compared to hydrogen. Therefore, Helium differs due to its two-electron structure.

Analysis of the permitted transitions in Helium (Table 5) confirmed some selection rules, where we note that Δn transitions occurred between a wide range of numbers, with no particular pattern, $|\Delta l|=1$ always, and $\Delta j = 0$ or ± 1 always. Furthermore, Table 5 revealed two distinct $n=3 \rightarrow 2$ transitions in helium ($1s3d \rightarrow 1s2p$ configurations). The multi-electron structure causes effects absent in hydrogen. While He^+ is hydrogen-like, neutral helium experiences electron-electron repulsion and spin effects that Bohr's model cannot account for. The successful measurement of reference lines for Helium, with all calibrated wavelengths within one error bar of their expected values, validates our calibration procedure, and was under 2% difference. The only expected wavelength that could not be measured was the one at 59 nm, which was not known on the spectrometer or the reference. This may be due to extremely small wavelengths or too low intensities to be detected by this device.

The unknown gas was identified as Krypton based on its spectral signature, with the strongest emission line at 751nm, and all the strongest wavelengths within 5% of Krypton's. The conclusion was based on the close match of its strongest emission lines (particularly in the 760-830nm range), where few other gases had these features, and a qualitative analysis of its visual colour (Appendix 2). The gas was also compared to the reference spectra from the software, which correlated most strongly with Argon and Xenon. We noted there may be discrepancies in the data because the spectrometer experiment itself has a lot of noise and randomness, as the light might be very faint compared to the stray lighting of the room. If this experiment were to be redone, it would be better conducted in a secluded dark room to increase the visibility of the light while ensuring safety for other experimenters, or we could determine the stray light ratio in our calibration of data using methods like the slit height method or Preston's method [10][11].

The dye analysis confirmed the complementary relationship between absorption and transmission, as the strongest transmission correlated to the colour emitted and the strongest absorption to the colour absorbed. A physically impossible negative transmittance value was recorded for one measurement (row 5), attributed to background noise or calibration drift at low signal levels. We also noted that the calculated reflectance values begin to deviate from the measured ones as the transmittance gets lower. This implies that the fewer the incident photons that are transmitted, the lower the accuracy of measuring the absorbance of the solution. Furthermore, the yellow dye's absorption edge was found at 387. ± 18. nm, corresponding to a band gap of around 3. eV. For photovoltaic applications, a narrower band gap (typically 1.4-2.1 eV) is desirable to absorb a broader range of the solar spectrum [13], which corresponds to absorption thresholds in the visible to near-infrared range. Since 3.0 eV lies above this optimal range, the dye is not suitable for use in photovoltaic cells. Limitations such as noisy fluorescence data and potential cuvette staining may have contributed to measurement uncertainty. It is also important to look at the bandwidths of the peaks because they can tell us the accuracy of the wavelength and can further increase or decrease the uncertainty and cause the type of gas being identified to change. A lower bandwidth is better because it has a lower wavelength variance [14].

In conclusion, the experiment validated quantum models for single-electron systems, highlighted their shortcomings for multi-electron atoms, and provided a practical application of emission spectroscopy for unknown gas identification. The analysis of dye solutions confirmed the principle of complementary colours in

absorption and transmission spectra. The primary limitations were systemic calibration errors, shown by high reduced chi-squared values and noise in optical measurements.

5. References

[1]J. Halpern, “6.3: Line Spectra and the Bohr Model,” Nov. 18, 2014. Available: https://chem.libretexts.org/Bookshelves/General_Chemistry/Map%3A_Chemistry_-_The_Central_Science_(Brown_et_al.)/06%3A_Electronic_Structure_of_Atoms/6.03%3A_Line_Spectra_and_the_Bohr_Model. [Accessed: Oct. 06, 2025]

[2]N. Krasnopolskaia, “Quantum States and Spectra of Gases.” in University of Toronto Physics Department. Sept. 2017. Available: https://www.physics.utoronto.ca/~phy224_324/LabManuals/OLD_Spectrometry.pdf

[3]“Interpreting the results of a Least Squares Fit.” Available: https://physics-50.github.io/General/DAG_interpreting-plots.html. [Accessed: Oct. 06, 2025]

[4]“Reduced chi-squared statistic.” Sept. 04, 2025. Available: https://en.wikipedia.org/w/index.php?title=Reduced_chi-squared_statistic&oldid=1309493339. [Accessed: Oct. 06, 2025]

[5]J. Strasser, H. Yersin, and H. H. Patterson, “Effect of high pressure on the emission spectrum of single crystals of Tl[Au(CN)2],” vol. 295, no. 1, pp. 95–98, Oct. 1998, doi: 10.1016/S0009-2614(98)00915-4. Available: https://www.sciencedirect.com/science/article/pii/S0009261498009154. [Accessed: Oct. 06, 2025]

[6]“Spectroscopy 101 – How Absorption and Emission Spectra Work - NASA Science,” Sept. 01, 2025. Available: https://science.nasa.gov/mission/webb/science-overview/science-explainers/spectroscopy-101-how-absorption-and-emission-spectra-work/. [Accessed: Oct. 06, 2025]

[7]C. Wang and C. Gu, *X-Ray Diffraction*. in Encyclopedia of Soils in the Environment (Second Edition). Oxford: Academic Press, 2023, pp. 642–653. Available: https://www.sciencedirect.com/science/article/pii/B9780128229743000379. [Accessed: Oct. 06, 2025]

[8] R. C. Massé and T. G. Walker, “Accurate energies of the He atom with undergraduate quantum mechanics,” 2015, doi: 10.1119/1.4921821. Available: https://pages.physics.wisc.edu/~tgwalker/118.HeAtom.pdf

[9] S. Mura, “Significance and Limitations of Bohr’s Atomic Model”, Available: https://www.walshmedicalmedia.com/open-access/significance-and-limitations-of-bohrs-atomic-model.pdf

[10]“Strong Lines of Argon (Ar).” Available: https://physics.nist.gov/PhysRefData/Handbook/Tables/argontable2_a.htm. [Accessed: Oct. 06, 2025]

[11] A. G. Reule, “Errors in Spectrophotometry and Calibration Procedures to Avoid Them,” no. 4, pp. 609–624, 1976, doi: 10.6028/jres.080A.060. Available: https://pmc.ncbi.nlm.nih.gov/articles/PMC5293527/. [Accessed: Oct. 06, 2025]

[12]A. G. Reule, “Errors in Spectrophotometry and Calibration Procedures to Avoid Them,” no. 4, pp. 609–624, 1976, doi: 10.6028/jres.080A.060. Available: https://pmc.ncbi.nlm.nih.gov/articles/PMC5293527/. [Accessed: Oct. 06, 2025]

[13]“How do we see colour?,” July 23, 2019. Available: https://letstalkscience.ca/educational-resources/stem-explained/how-do-we-see-colour#:~:text=What%20Is%20Colour. [Accessed: Oct. 06, 2025]

[14]H. Becker-Roß, S. Florek, U. Heitmann, and R. Weiße, “Influence of the spectral bandwith of the spectrometer on the sensitivity using continuum source AAS,” vol. 355, no. 3, pp. 300–303, June 1996, doi: 10.1007/s0021663550300. Available: https://doi.org/10.1007/s0021663550300. [Accessed: Oct. 06, 2025]

Appendix 1: Materials

Opens the file structure of the software to Open, Create and Save the *.sp files.

Analyze Light in terms of Intensity vs Wavelength:
Yellow - "Currently in use";
White – Not in use, but available for use;
Grey – disabled (e.g. the spectrometer is not turned on).

Analyze a gas or a solution spectrum in terms of Absorbance, Transmittance and/or Fluorescence vs wavelength.

Analyze a Solution in terms of Absorbance, Transmittance and/or Fluorescence vs solution concentration. Not in use in PHY293Lab.

Analyze a Solution in terms of Absorbance, Transmittance, Fluorescence and/or concentration vs reaction time. Not in use in PHY293Lab.

Connection Status:
Error

OR

Connected

Take Journal Snapshot

Show Journal Snapshots

Software information and settings

Export Snapshots To HTML:
Sharing Options (Tablet only)
Open in another app: save the *.sp file into Google Drive, DropBox, etc. that are installed on the device.

Integration Time

With a higher integration time, the spectrometer is more sensitive to less intense light.
The "Auto Set" button automatically adjusts the integration time to maximize the spectrum.

Number of Scans to Average

The higher number of scans results in a better the signal-to-noise ratio. Should be adjusted manually for each spectrum.

Smoothing

Average groups of adjacent data points. May change the shape of the spectrum drastically. Not always recommended to exceed 1.

Absorbance/Transmittance	Analyze absorbance and transmittance of a white light source through the sample. Select “Absorbance” on the graph to switch from Absorbance to Transmittance.
Fluorescence (405 nm)	Analyze fluorescence of the sample with 405-nm excitation.
Fluorescence (500 nm)	Analyze fluorescence of the sample with 500-nm excitation.

Calibrate Dark.

Calibrate Reference (e.g. distilled water in a cuvette if it is a solvent of the unknown solution).

Show dual Y-axes of absorbance and transmittance data only.

Appendix 2: Xenon and Argon Graphs

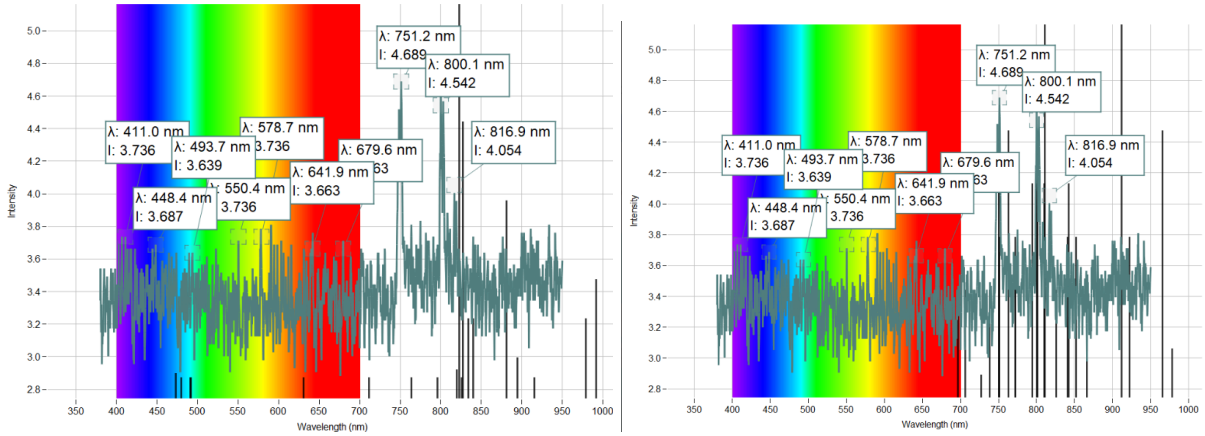

Figure 6: Figure 6 compares the spectra of our unknown gas to reference spectra for Argon (left) and Xenon (right). While there was some overlap, the alignment was not conclusive, prompting the hypothesis that Krypton, another noble gas not available in the PASCO reference library, might provide a better match.

Appendix 3: Qualitative Unknown Gas Analysis

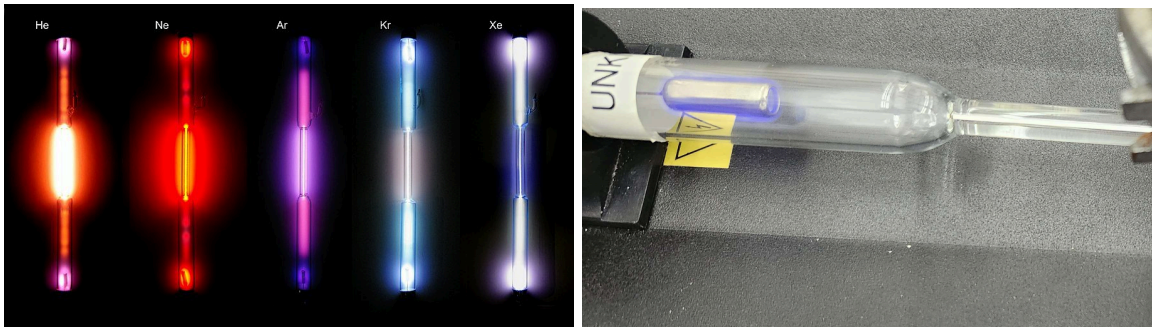

Figure 7: A Qualitative Comparison between the emission colours of our unknown gas with various noble gases that have similar 'strongest spectral lines'. For this, it can be narrowed down that the unknown gas may be Xenon or Krypton.

Appendix 4: Error Propagation from Calibration

The origin of error for the experimental wavelengths is from the linear fit in Section 1. The error, therefore in λ_{true} is from uncertainty in slope m, uncertainty in intercept b, and the spectrometer resolution (2-3nm), giving a total error of $\sigma_{true} = \sqrt{(\lambda_{measured} * \sigma_m)^2 + (\sigma_b)^2 + (m * \sigma_{resolution})^2}$, choosing the error of the resolution to be the maximum, which is 3nm.

Appendix 5: Helium Spectroscopy

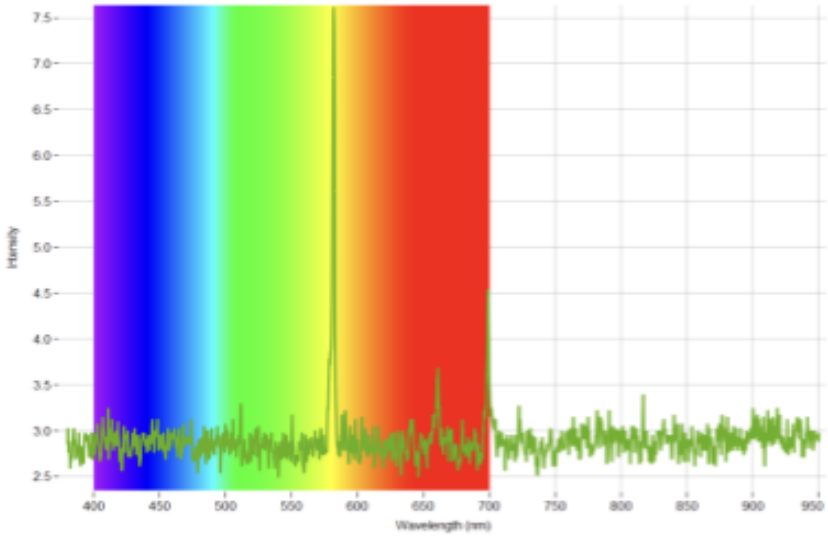

Figure 4: Emission lines of the Helium atom.

Appendix 6: Code

https://github.com/sarapr06/PHY293-W1-lab-Quantum-Spectra